

Comparison of Dynamic Hardening Equations for Metallic Materials with the Variation of Crystalline Structures

K. Ahn¹, H. Huh¹, L. Park²

¹ KAIST, Daejeon, Korea

² ADD, Daejeon, Korea

Abstract

This paper is concerned with dynamic hardening equations of metallic materials with various crystalline structures. The dynamic response of metallic materials is indispensable for analysis of high speed metal forming process. There is, however, no unique equation which can represent the dynamic hardening characteristics of all kinds of materials although various dynamic hardening equations have been suggested by many researchers. Dynamic hardening equations reported have been investigated using the dynamic hardening characteristics of three kinds of materials: 4340Steel (BCC); OFHC (FCC); and Ti6Al4V (HCP). Dynamic hardening characteristics of each material have been obtained by uniaxial tensile tests and SHPB tests. Uniaxial tensile tests have been performed with the variation of the strain rate from 0.001/sec to 100/sec and SHPB tests have been conducted at the strain rate ranged up to 4000/sec. Several existing models have been constructed and evaluated for Johnson-Cook model, Zerilli-Armstrong model, Preston-Tonks-Wallace model, modified Johnson-Cook model, and modified Khan-Huang model using test results of three materials. Strain rate hardening and thermal softening effect during the deformation process were investigated for accurate application of hardening equations. The most applicable equation for each material has been suggested by comparison of constructed results.

Keywords

Dynamic hardening equation, Strain rate sensitivity, High speed tensile test

1 Introduction

The deformation behavior of metallic materials at high strain rates has been investigated for the past several decades and high speed forming is the recent megatrend especially for automobile industries, defense industries and so on. Accurate understanding of material properties at various strain rates is necessary to guarantee the reliability of the analysis at high speed conditions such as high speed forming and deformation analysis. When a metallic material deforms under the dynamic loading, the inertia effect and the stress wave

propagation become so important that the material properties are remarkably changed by the level of the strain rate. It is well-known that the flow stress of a material increases as the strain rate increases and this tendency is regarded as the inherent characteristics of the material. Although the dynamic characteristics of the metallic materials such as steel, aluminum and copper have been the challenging issue of extensive studies experimentally and theoretically [1], there is no unique equation which can represent the dynamic hardening characteristics of all kinds of materials. The quantification of the dynamic hardening characteristics using the dynamic hardening equation is very important and convenient to represent flow stress–strain relation of material. Various dynamic hardening equations have been suggested by many researchers to represent the dynamic hardening characteristics of metallic material using one simple equation.

In this paper, dynamic hardening equations reported have been investigated using the dynamic hardening characteristics of three kinds of materials: 4340Steel (BCC); OFHC (FCC); and Ti6Al4V (HCP) in order to suggest the most applicable dynamic hardening equation in view of the crystalline structures of materials. Dynamic hardening characteristics of each material have been obtained by uniaxial tensile tests and SHPB tests. Uniaxial tensile tests have been performed at the strain rate ranging from 0.001/sec to 100/sec and SHPB tests have been conducted at the strain rate ranged up to 4000/sec. Several existing models have been constructed from the test results and investigated for applicability with Johnson-Cook model [2], Zerilli-Armstrong model [3], and Preston-Tonks-Wallace model [4] using test results of three materials. Modified Johnson-Cook model [5] and modified Khan-Huang model [6,7] suggested have been also constructed from the test results for accurate quantification of hardening characteristics. Strain rate hardening and thermal softening effect during the deformation process were investigated for accurate hardening equations. The most applicable equation for each material has been suggested by comparison of constructed results.

2 Review of Dynamic Hardening Equations

Various dynamic hardening equations have been suggested to represent the effects of strain, strain rate, and temperature on the hardening characteristics of metallic materials. In this chapter, Johnson-Cook model, Zerilli-Armstrong model, Preston-Tonks-Wallace model, modified Johnson-Cook model, and modified Khan-Huang model have been used for the review and quantification of dynamic hardening characteristics of three kinds of materials of BCC, FCC, and HCP.

2.1 Johnson-Cook Model

Johnson-Cook model [2] was proposed to represent the effect of strain, strain rate, and temperature on the flow stress of metallic materials as below:

$$\sigma = \left[A + B\varepsilon^n \right] \left[1 + C \ln \frac{\dot{\varepsilon}}{\dot{\varepsilon}_0} \right] \left[1 - \left(\frac{T - T_r}{T - T_m} \right)^m \right] \quad (1)$$

where ε is the equivalent plastic strain, $\dot{\varepsilon}/\dot{\varepsilon}_0$ is the dimensionless plastic strain rate for $\dot{\varepsilon}_0=1/\text{sec}$, T_r, T_m is the room temperature and the melting temperature of the material,

respectively. The five constants are adopted with A , B , n , C , and m . The expression in the first term of brackets gives the stress as a function of strain for $\dot{\varepsilon}=1/\text{sec}$ and $T=T_r$. The expression in the second and third terms of brackets represents the effects of strain rate and temperature, respectively. This model is the most widely used model due to its simplicity, but it has some shortcomings to represent the hardening characteristics of all kinds of materials. Strain rate hardening term in the second term is expressed as a linear function of the logarithm of strain rate. This expression cannot represent accurate initial yield stress at various strain rates due to the strain rate change in general metallic materials. Because of linear expression of strain rate hardening, linear relation of initial yield stress is predicted with the change of logarithm of strain rate. This is not valid in all actual cases for general metallic materials.

2.2 Zerilli-Armstrong Model

Zerilli-Armstrong model [3] suggests different expression for FCC and BCC materials based on the dislocation dynamics.

$$\begin{aligned}\sigma &= C_0 + [C_1 + C_2\sqrt{\varepsilon}] \exp[-C_3T + C_4T \ln \dot{\varepsilon}] + C_5\varepsilon^n \\ \text{for FCC } (C_1 = C_5 = 0): \sigma &= C_0 + C_2\sqrt{\varepsilon} \exp[-C_3T + C_4T \ln \dot{\varepsilon}] \\ \text{for BCC } (C_2 = 0) \quad : \sigma &= C_0 + C_1 \exp[-C_3T + C_4T \ln \dot{\varepsilon}] + C_5\varepsilon^n\end{aligned}\quad (2)$$

where C_0 , C_1 , C_2 , C_3 , C_4 , C_5 are material constants. C_0 is related to Hall-Petch relation as $C_0 = \Delta\sigma'_G + kd^{-\frac{1}{2}}$. Zerilli-Armstrong model suggests two different expressions using the hardening characteristics with the variation of crystalline structures of materials. In the FCC case, main consideration is that the temperature softening and strain rate hardening dependence of flow stress are greater with increased strain hardening. In the BCC case, strain hardening factor is uncoupled from the strain rate hardening and thermal softening. From the expression of two different Zerilli-Armstrong models, a shortcoming for each model can be discussed. In the FCC case, C_0 is independent of strain rate and temperature. This expression induces the constant yield stress with the change of strain rate and temperature. With that expression, FCC model cannot represent the change of the initial yield stress with the change of strain rate and temperature. In the BCC case, strain hardening factor of $C_5\varepsilon^n$ is uncoupled from the strain rate hardening and thermal softening term. Due to this expression, BCC model cannot represent the hardening change with the change of strain rate and temperature.

2.3 Preston-Tonks-Wallace Model

Thermal activation mechanism is known to predominate the deformation mechanism at the strain rate ranged up to $10^5/\text{sec}$. Preston-Tonks-Wallace model [4] extends the Mechanical Threshold Stress model [8](valid for $\dot{\varepsilon} < 10^5/\text{sec}$) to the strain rate ranged up to $10^{12}/\text{sec}$. Preston-Tonks-Wallace model suggests two different hardening characteristics at thermal regime($\dot{\varepsilon} < 10^5/\text{sec}$) and dislocation–drag dominated shock regime($10^9 < \dot{\varepsilon} < 10^{12}/\text{sec}$), respectively. The gap between two regimes is represented as the maximum value of the hardening expression in two regimes without introducing any additional material parameters.

Preston-Tonks-Wallace model can be represented as below:

- At thermal regime ($\dot{\varepsilon} < 10^5$ / sec)

$$: \hat{\tau} \cong \tau_s + \frac{1}{p}(s_0 - \tau_y) \ln \left[1 - \left[1 - \exp\left(-p \frac{\hat{\tau}_s - \tau_y}{s_0 - \tau_y}\right) \right] \times \exp \left\{ -\frac{p\theta\psi}{(s_0 - \hat{\tau}_y) \left[\exp\left(-p \frac{\hat{\tau}_s - \tau_y}{s_0 - \tau_y}\right) - 1 \right]} \right\} \right] \quad (3)$$

- At shock regime ($10^9 < \dot{\varepsilon} < 10^{12}$ / sec)

$$: \hat{\tau}_s = \tau_y = \text{constant} \times (\dot{\psi} / \dot{\varepsilon})^\beta$$

where $\hat{\tau}$ is the normalized flow stress ($\hat{\tau} = \tau / G$ where τ is the shear stress and G is the shear modulus), and $\hat{\tau}_s$, $\hat{\tau}_y$ are the normalized work hardening saturation stress and normalized shear stress, respectively. ψ is plastic strain and the variables, p , θ , and s_0 are dimensionless material constants. $\hat{\tau}_s$ and $\hat{\tau}_y$ are represented as

$$\hat{\tau}_s = s_0 - (s_0 - s_\infty) \text{erf} \left[\kappa \hat{T} \ln(\gamma \dot{\varepsilon} / \dot{\psi}) \right] \quad (4)$$

$$\hat{\tau}_y = y_0 - (y_0 - y_\infty) \text{erf} \left[\kappa \hat{T} \ln(\gamma \dot{\varepsilon} / \dot{\psi}) \right] \quad (5)$$

where the material constants s_0 and s_∞ are the values of $\hat{\tau}_s$ at the absolute zero temperature and very high temperature, respectively. y_0 and y_∞ have analogous interpretations. κ and γ are dimensionless material constants. Scaled temperature \hat{T} is defined by T/T_m where T_m is the melting temperature. $\dot{\psi} / \gamma \dot{\varepsilon}$ is the dimensionless strain rate variable.

Since this paper deals with the hardening characteristics of metallic materials at the strain rate range up to 4000/sec, Preston-Tonks-Wallace model at shock regime has not been constructed.

2.4 Modified Johnson-Cook Model

Modified Johnson-Cook model [5] is developed by modification of the strain rate hardening term of Johnson-Cook model. Linear expression of strain rate hardening term in Johnson-Cook model is substituted by the exponential expression as below:

$$\sigma = \left[A + B\varepsilon^n \right] \left[1 + C \left(\ln \frac{\dot{\varepsilon}}{\dot{\varepsilon}_0} \right)^p \right] \left[1 - \left(\frac{T - T_r}{T - T_m} \right)^m \right] \quad (6)$$

where $\dot{\varepsilon}_0 = 0.001$ /sec (reference strain rate). General metallic materials show the exponential relation of the initial yield stress to the logarithm of strain rate. Modified Johnson-Cook model can represent the yield stress change with respect to the strain rate more

accurately than Johnson-Cook model. Modified Johnson-Cook model, however, still express the flow stress change with respect to strain rate by simple scaling of strain hardening curve at the reference strain rate(0.001/sec). It shows deviation from dynamic characteristics of general metallic materials.

2.5 Modified Khan-Huang Model

Khan-Huang model [9] is suggested to describe the change of strain hardening due to the change of strain rate.

$$\sigma = \left[A + B \left(1 - \frac{\ln \dot{\epsilon}}{\ln D_0^p} \right)^{n_1} \epsilon^{n_0} \right] e^{C \ln \dot{\epsilon}} \left[1 - \left(\frac{T - T_r}{T - T_m} \right)^m \right] \quad \text{where } D_0^p = 10^6 / \text{sec} \quad (7)$$

Strain hardening term in the first bracket is described by function of strain and strain rate which can induce the increase or decrease of strain hardening due to the change of strain rate. Modified Khan-Huang model [6] is suggested by modification of the strain rate hardening term in Khan-Huang model as done in modified Johnson-Cook model.

$$\sigma = \left[A + B \left(1 - \frac{\ln \dot{\epsilon}}{\ln D_0^p} \right)^{n_1} \epsilon^{n_0} \right] \left[1 + C \left(\ln \frac{\dot{\epsilon}}{\dot{\epsilon}_0} \right)^p \right] \left[1 - \left(\frac{T - T_r}{T - T_m} \right)^m \right] \quad \text{where } D_0^p = 10^9 / \text{sec} \quad (8)$$

3 Experiments

Dynamic hardening characteristics of three kinds of materials: 4340Steel (BCC); OFHC (FCC); Ti6Al4V (HCP) have been obtained by uniaxial tensile tests and SHPB tests. Uniaxial tensile tests at the quasi-static strain rate(0.001~0.01/sec) have been conducted using INSTRON5583 Universal Testing Machine. A servo-hydraulic type high speed material testing machine is used for the dynamic material tests at the intermediate strain rates ranging from 0.1 to 100/sec. A split Hopkinson pressure bar has been used for the tests at the strain rates over 1000/sec.

3.1 Dynamic Tensile Tests at Intermediate Strain Rates

A servo-hydraulic type high speed material testing machine is utilized for the dynamic material test at intermediate strain rates [10,11]. The maximum velocity and load of the apparatus are 7800 mm/s and 30 kN, respectively. The load is acquired from a piezoelectric-type load cell and the displacement is obtained from an LDT(linear displacement transducer). The machine is equipped with a gripper fixture specially designed to obtain the constant tensile velocity during the test and to reduce the noise in data acquisition from the load cell. The high speed material testing machine and the specimen used in the experiment are illustrated in Figure 1. The dimension of a specimen is determined from finite element analysis for the gauge section to be uniformly elongated at intermediate strain rate [12].

Tensile tests were conducted for the three materials at the strain rate ranged from 0.1/sec to 100/sec. Tensile tests at the quasi-static state from 0.001 to 0.01/sec were conducted using the UTM. Tests were repeated five times for each condition. Stress–strain curves of three materials are obtained at various strain rates as shown in Figure 2. Test

results show that the flow stress is influenced by the strain rate for three materials.

3.2 Hopkinson Bar Tests at High Strain Rates

The dynamic responses of the three materials at high strain rates were obtained from the split Hopkinson pressure bar test using disc type specimens whose diameter and thickness are 10 mm and 5 mm, respectively [13]. This split Hopkinson pressure bar is a very popular experimental technique for identification of dynamic material characteristics at high strain rates. Stress–strain curves at the high strain rate are acquired by measuring the stress waves propagating through the incident and the transmitted bar in this apparatus.

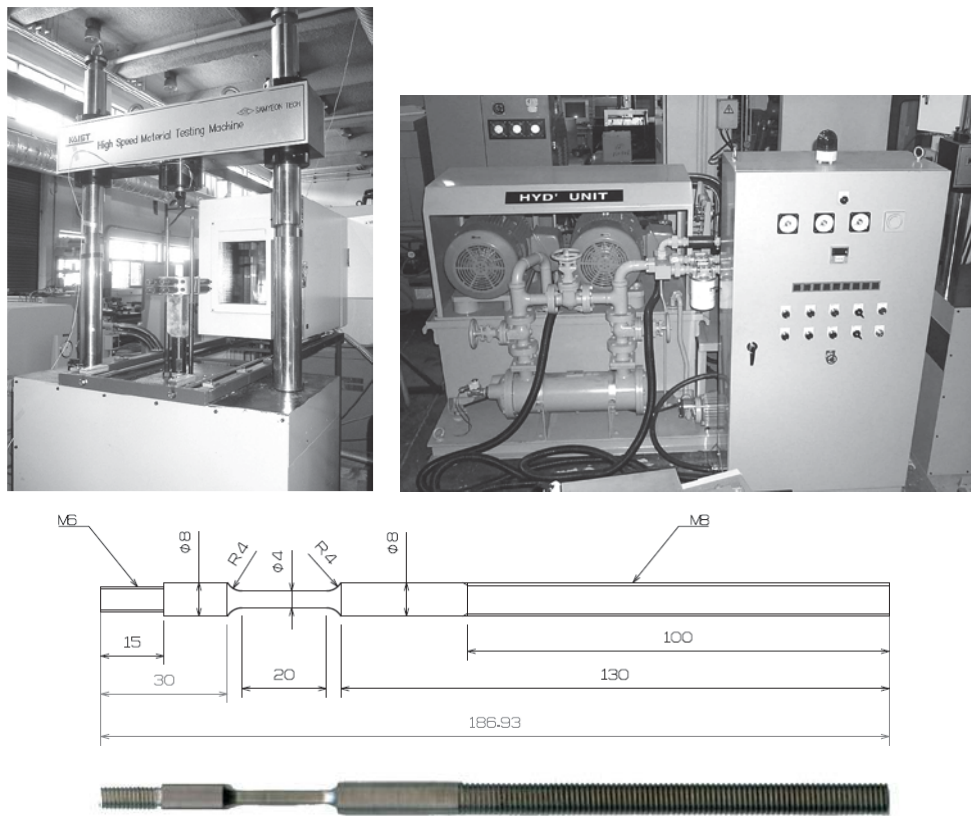


Figure 1: High speed material testing machine and dimension of specimen

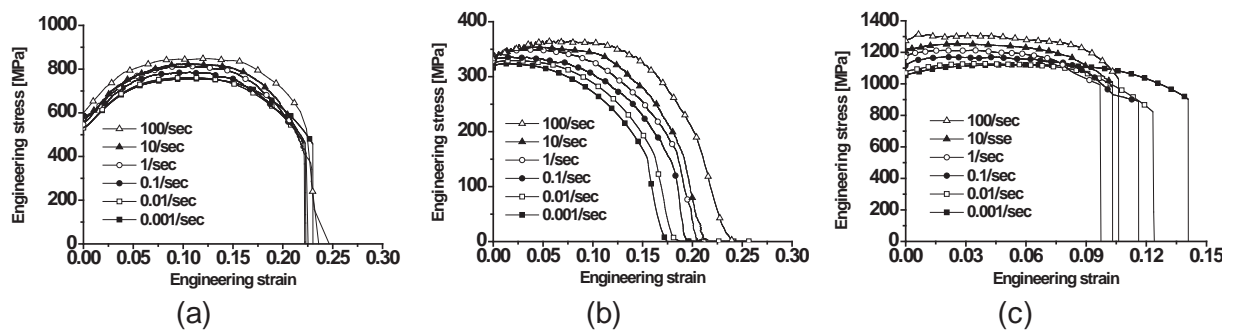


Figure 2: Engineering stress–strain curves at various strain rates: (a) 4340Steel (BCC); (b) OFHC (FCC); (c) Ti6Al4V (HCP)

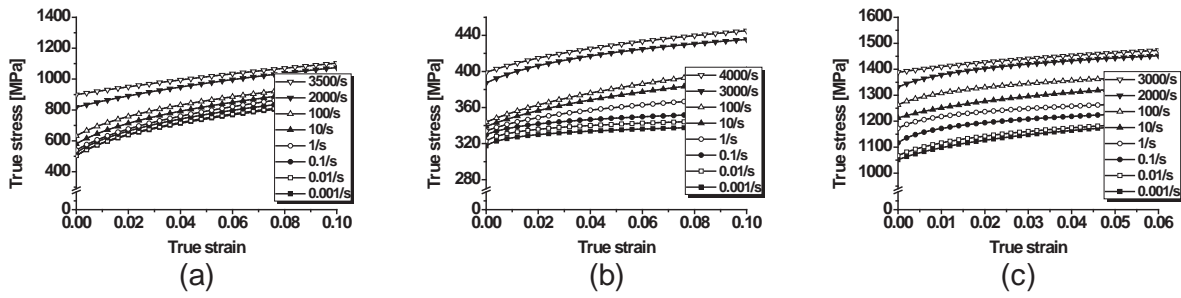


Figure 3: True stress–strain curves at various strain rates: (a) 4340Steel (BCC); (b) OFHC (FCC); (c) Ti6Al4V (HCP)

4 Model Construction

Figure 3 shows true stress–strain curves of the three materials at strain rates ranged from 0.001/sec to 4000/sec. Each data was obtained by fitting the experimental results using the data up to the ultimate tensile strength. Six dynamic hardening equations introduced in the previous chapter have been constructed using true stress–strain data in Figure 3. For the sake of accuracy, true strain rate and thermal softening effects were introduced since the strain rate and temperature change during the test. A strain rate can be expressed as equation (9) where V is the tensile speed and L_0 is the gauge length. During the test, the gauge length of a specimen changes continuously and so does the strain rate. The strain rate during the tensile test reduces as an exponential function of equation (10) [14]. Temperature of the specimen also changes during the test. At high strain rate conditions ($\dot{\varepsilon} \geq 0.01/\text{sec}$), 90% of the plastic deformation energy is converted to heat energy. This relation can be expressed as equation (11).

$$\dot{\varepsilon} = V/L_0 \quad (9)$$

$$\dot{\varepsilon}_{true} = (V/L_0)\exp(-\varepsilon) \quad (10)$$

$$\Delta T = \frac{0.9}{\rho C} \int_0^\varepsilon \sigma(\varepsilon) d\varepsilon \quad (11)$$

In this study, strain rate and temperature change during the tests were considered for more accurate model construction.

It is important to represent the initial yield stress change with respect to the strain rate accurately since the yield stress indicates the onset of plastic deformation. Figures 4 to 6 show comparison of the initial yield stress from experiments with that of each model for the three materials. Johnson-Cook model cannot represent the initial yield stress change accurately due to its linear expression of the strain rate hardening term. Zerilli-Armstrong for FCC model represents constant yield stress. Preston-Tonks-Wallace model uses the error function and Zerilli-Armstrong for BCC model uses exponential function for the representation of the initial yield stress change. Modified Johnson-Cook model and modified Khan-Huang model use exponential function of the logarithm of strain rate and they show the best fit for the initial yield stress change with respect to the strain rate.

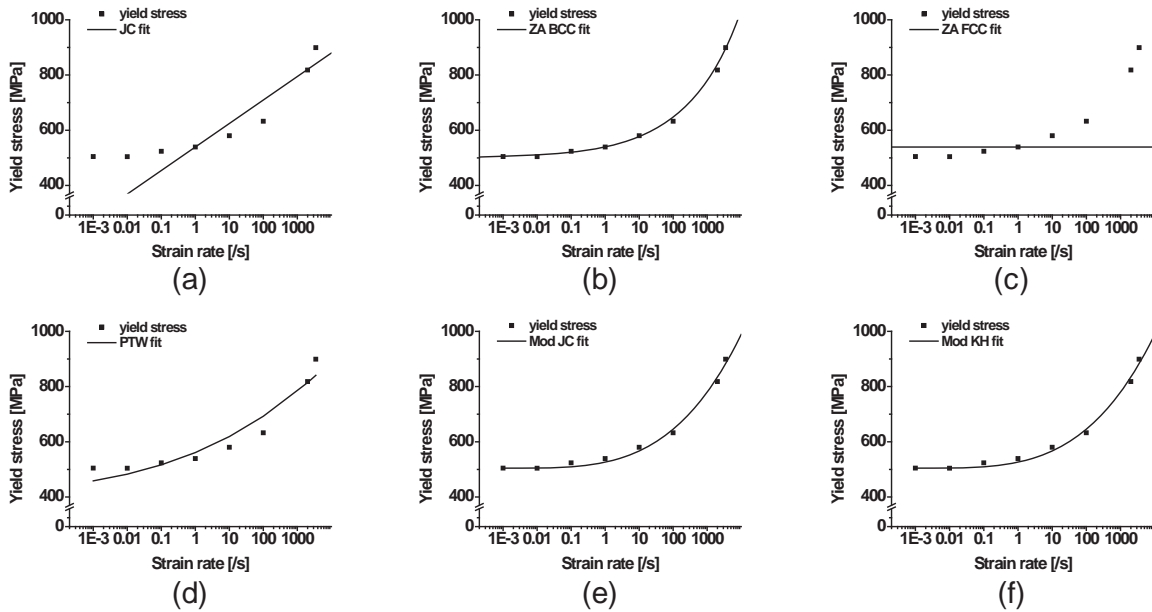


Figure 4: Representation of yield stress change of 4340Steel(BCC) with respect to strain rate: (a) JC; (b) ZA BCC; (c) ZA FCC; (d) PTW; (e) Mod JC; (f) Mod KH

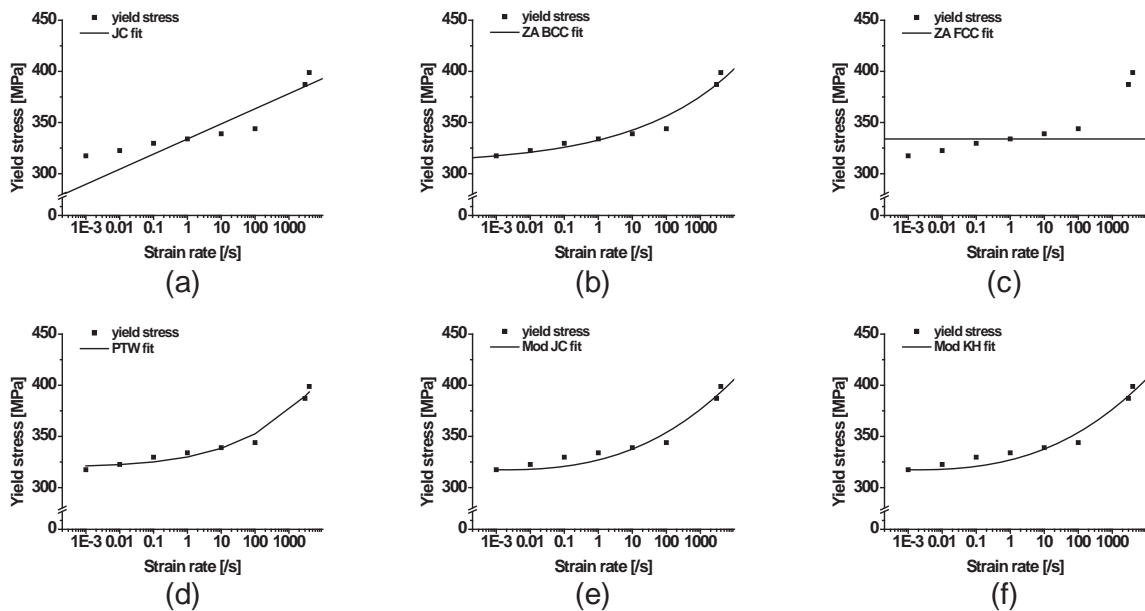


Figure 5: Representation of yield stress change of OFHC(FCC) with respect to strain rate: (a) JC; (b) ZA BCC; (c) ZA FCC; (d) PTW; (e) Mod JC; (f) Mod KH

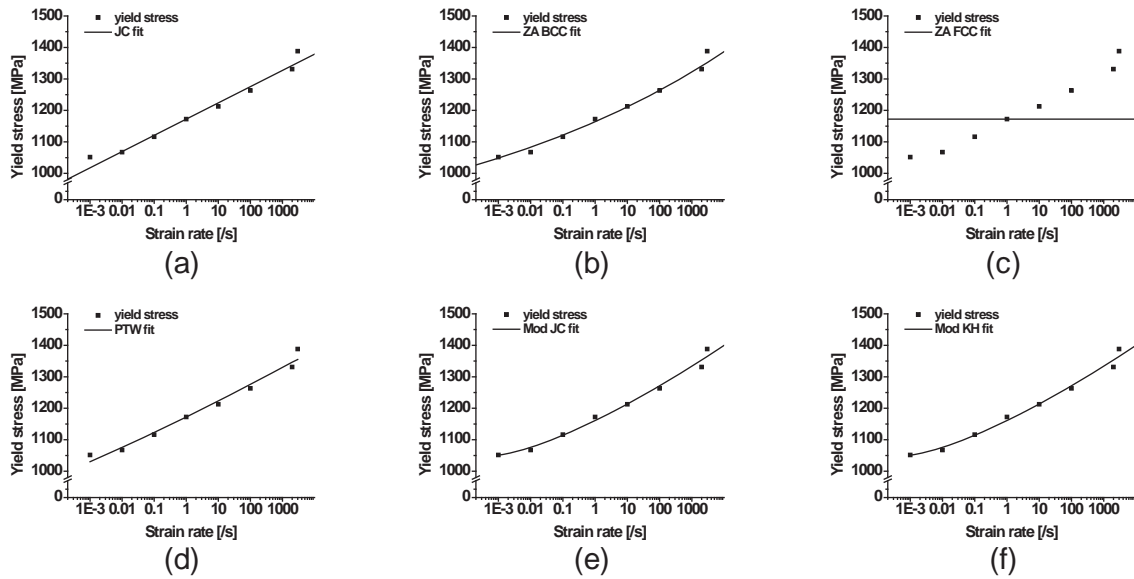


Figure 6: Representation of yield stress change of Ti6Al4V(HCP) with respect to strain rate: (a) JC; (b) ZA BCC; (c) ZA FCC; (d) PTW; (e) Mod JC; (f) Mod KH

Figures 7 to 9 show the comparison of hardening from experiments with hardening representation of each model for the three materials. Both Johnson-Cook model and Zerilli-Armstrong for FCC model show noticeable deviation for hardening characteristics due to their improper expression of the yields stress. Modified Johnson-Cook model also shows large deviation since the flow stress change in the model is expressed by simple scaling of the flow stress at the reference strain rate. Zerilli-Armstrong for BCC model cannot represent the hardening change with respect to the strain rate. Preston-Tonks-Wallace model is the best model for OFHC(FCC) and modified Khan-Huang model is the best model for 4340Steel(BCC) and Ti6Al4V(HCP) since those models can represent the accurate initial yield stress and hardening change with respect to the strain rate.

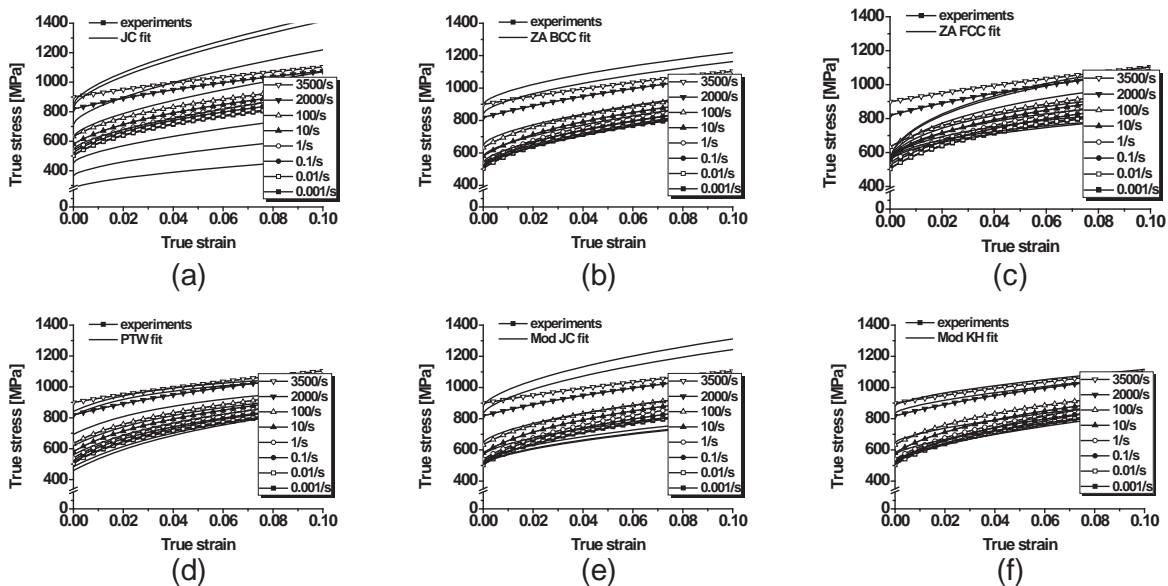


Figure 7: Representation of hardening change of 4340Steel(BCC) with respect to strain rate: (a) JC; (b) ZA BCC; (c) ZA FCC; (d) PTW; (e) Mod JC; (f) Mod KH

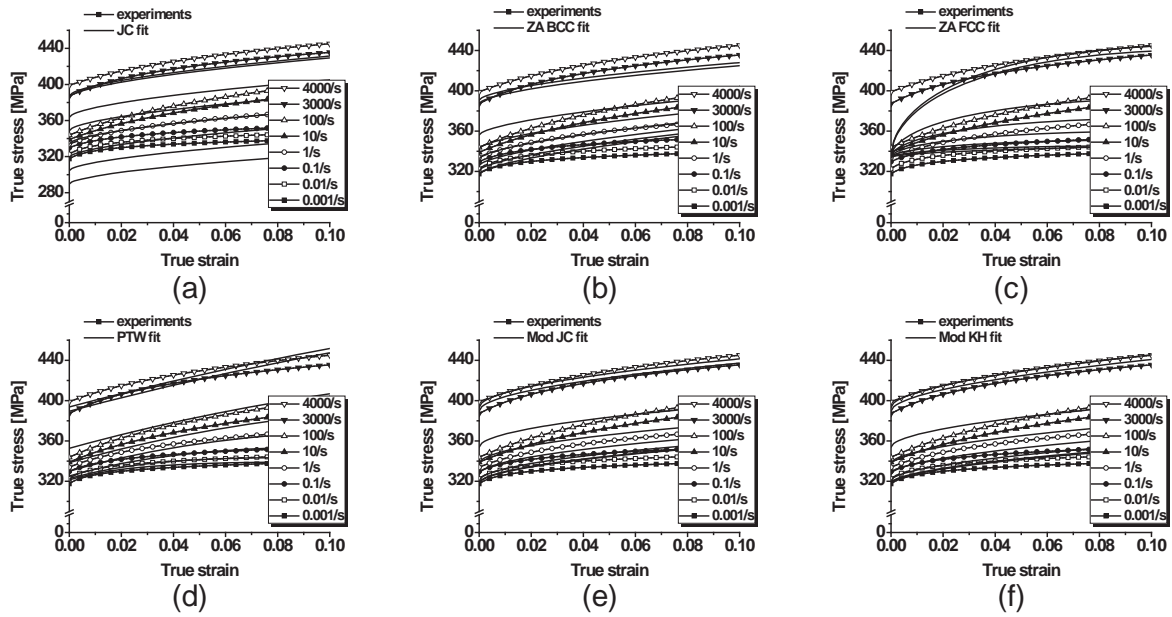


Figure 8: Representation of hardening change of OFHC(FCC) with respect to strain rate: (a) JC; (b) ZA BCC; (c) ZA FCC; (d) PTW; (e) Mod JC; (f) Mod KH

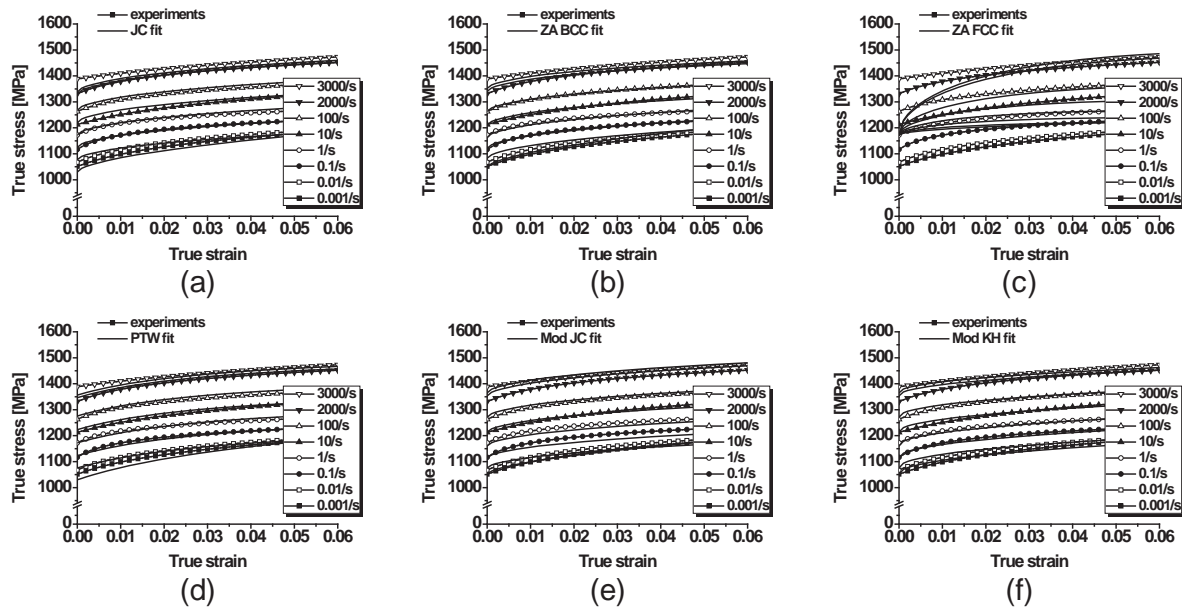


Figure 9: Representation of hardening change of Ti6Al4V(HCP) with respect to strain rate: (a) JC; (b) ZA BCC; (c) ZA FCC; (d) PTW; (e) Mod JC; (f) Mod KH

Figure 10 shows the quantitative evaluation of each model for both the initial yield stress and hardening representation. For all kinds of materials, Johnson-Cook and Zerilli-Armstrong for FCC model induce large deviation for the initial yield stress and hardening representation. Modified Johnson-Cook model is enhanced for the yield stress representation although hardening representation still shows improper results. Zerilli-Armstrong for BCC model can represent the accurate hardening characteristics of a material when hardening does not show much change with respect to the strain rate like Ti6Al4V. Preston-Tonks-Wallace and modified Khan-Huang model can represent the change of hardening and the initial yield stress accurately. Figure 11 shows the material coefficients for each model constructed.

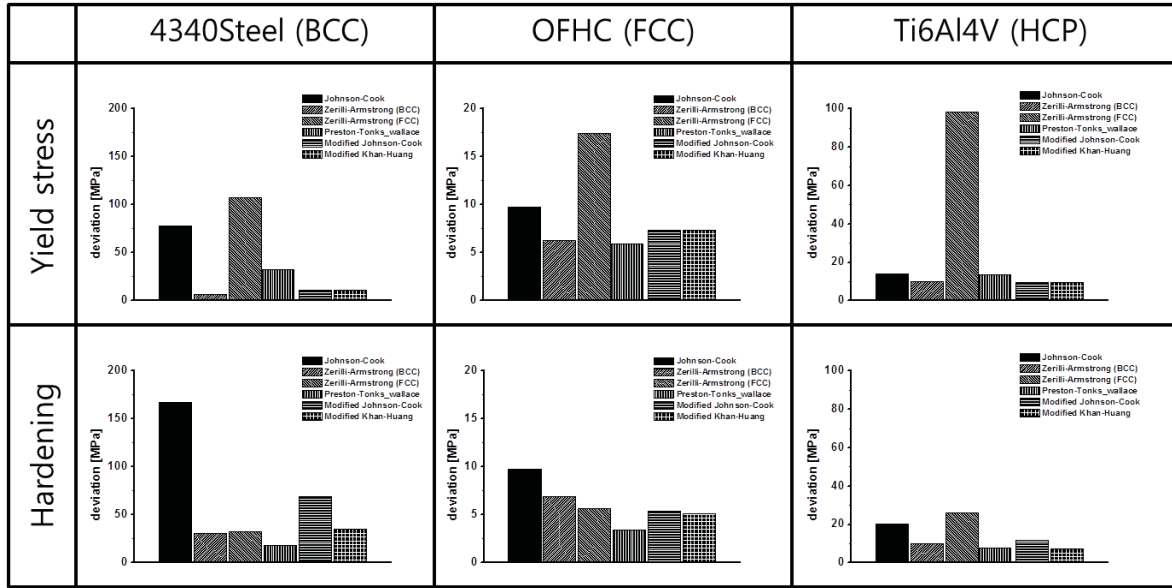


Figure 10: Quantitative evaluation of each constructed results

Johnson-Cook model coefficients					
	A	B	n	C	m
4340Steel	539	1632	0.629	0.069	0.350
OFHC	334	147	0.583	0.019	0.565
Ti6Al4V	1172	298	0.398	0.019	1.500

Zerilli-Armstrong for BCC model coefficients						
	C ₀	C ₁	C ₃	C ₄	C ₅	n
4340Steel	528	1280	0.016	0.001	1136	0.514
OFHC	309	986	0.012	4.93X10 ⁻⁴	193	0.638
Ti6Al4V	737	1581	0.004	1.52X10 ⁻⁴	914	0.605

Zerilli-Armstrong for FCC model coefficients				
	C ₀	C ₂	C ₃	C ₄
4340Steel	539	12594	0.008	1.98X10 ⁻⁴
OFHC	334	9.32X10 ⁶	0.038	5.74X10 ⁻⁴
Ti6Al4V	1172	37296	0.014	4.66X10 ⁻⁴

Preston-Tonks-Wallace model coefficients								
	y ₀	y _∞	k	γ	p	θ	s ₀	s _∞
4340Steel	0.012	0.003	0.308	0.001	2	0.053	0.007	0.007
OFHC	0.010	0.004	0.335	0.001	12	0.009	0.048	0.004
Ti6Al4V	0.020	0.005	0.114	0.001	15	0.066	0.032	0.019

Modified Johnson-Cook model coefficients						
	A	B	n	C	p	m
4340Steel	504	1591	0.637	3.66X10 ⁻⁵	3.660	0.478
OFHC	317	128	0.519	1.81X10 ⁻⁴	2.641	2.756
Ti6Al4V	1051	613	0.536	0.007	1.366	0.744

Modified Khan-Huang model coefficients							
	A	B	n ₁	n ₀	C	p	m
4340Steel	504	1946	0.911	0.651	3.66X10 ⁻⁵	3.660	6.025
OFHC	317	123	-0.132	0.543	1.81X10 ⁻⁴	2.641	6.500
Ti6Al4V	1051	448	0.388	0.459	0.007	1.366	6.516

Figure 11: Material coefficients for each constructed model

5 Conclusions

This paper is concerned with the characteristics of various dynamic hardening equations in view of the dynamic behavior of the three kinds of materials. The dynamic response at the intermediate strain rate is obtained from the high speed tensile test and that at the high strain rate from the split Hopkinson pressure bar test. It is important to investigate the initial yield stress and the hardening characteristics of each dynamic hardening equation in order to quantify the dynamic hardening characteristics of metallic materials. Four kinds of famous dynamic hardening equations were investigated and evaluated for its applicability. Two kinds of modified dynamic hardening equations developed by KAIST were also investigated. Preston-Tonks-Wallace model is the best model for OFHC(FCC), and modified Khan-Huang model is the best model for 4340Steel(BCC) and Ti6Al4V(HCP). Johnson-Cook model and Zerilli-Armstrong model have significant shortcomings in representation of the initial yield stress and hardening characteristics. Modified Johnson-Cook model also shows improper results for hardening characteristics. Zerilli-Armstrong for BCC model is limited for the

material in which hardening does not change with respect to the strain rate. Modified Khan-Huang model and Preston-Tonks-Wallace model afford good representation of the initial yield stress and the hardening change with respect to the strain rate.

References

- [1] *Mayers M.*: Dynamic Behavior of Materials. John Wiley & Sons, New York. 1994.
- [2] *Johnson G. R.; Cook W. H.*: A constitutive model and data for metals subjected to large strains, high strain rates and high temperatures. Proceedings of the Seventh International Symposium on Ballistics, The Hague, The Netherland, 1983, p.541-547.
- [3] *Zerilli F. J.; Armstrong R. W.*: Dislocation-mechanics-based constitutive relations for material dynamics calculations. Journal of Applied Physics, Vol.61, 1987, p.1816-1825.
- [4] *Preston D. L.; Tonks D. L.; Wallace D. C.*: Model of plastic deformation for extreme loading conditions. Journal of Applied Physics, Vol.93, 2003, p.211-220.
- [5] *Kang W. J.; Cho S. S.; Huh H.; Chung D. T.*: Modified Johnson-Cook model for vehicle body crashworthiness simulation. International Journal of Vehicle Design, Vol.21, 1999, p.424-435.
- [6] *Lee H. J.; Song J. H.; Huh H.*: Dynamic tensile tests of auto-body steel sheets with the variation of temperature. Solid State Phenomena, Vol.116-117, 2006. p.259-262.
- [7] *Huh H.; Lee H. J.; Song J. H.*: Dynamic hardening equation of the auto-body steel sheet with the variation of temperature. International Journal of Automotive Technology, Vol.13, 2012. p.43-60.
- [8] *Follansbee P. S.; Kocks U. F.*: A constitutive description of the deformation of copper based on the use of the mechanical threshold stress as an internal state variable. Acta Metallurgica, Vol.36, 1988, p.81-93.
- [9] *Khan A. S.; Huang S.*: Experimental and theoretical study of mechanical behavior of 1100 aluminum in the strain rate range 10^{-5} - 10^4 s⁻¹. International Journal of Plasticity, Vol. 8, 1992, p.397-424.
- [10] *Huh H.; Lim J. H.; Park S. H.*: High speed tensile test of steel sheets for the stress-strain curve at the intermediate strain rate. International Journal of Automotive Technology, Vol.10, 2009, p.195-204.
- [11] *Huh H.; Kim S. B.; Song J. H.; Lim J. H.*: Dynamic tensile characteristics of TRIP-type and DP-type steel sheets for an auto-body. International Journal of Mechanical Sciences, Vol.50, 2008, p.918-931.
- [12] *Song J. H.; Huh H.*: Dynamic material property of the sinter-forged Cu-Cr alloys with the variation of chrome content. Transactions of KSME(A), Vol.30, 2006, p.670-677.
- [13] *Huh H.; Kang W. J.; Han S. S.*: A tension split Hopkinson bar for investigating the dynamic behavior of sheet metals. Experimental Mechanics, Vol.42, 2002, p.8-17.
- [14] *Gao Y.; Wagoner R. H.*: A simplified model of heat generation during the uniaxial tensile test. Metallurgical Transactions A, Vol.18A, 1987, p.1001-1009.